Protein Nanosheet Mechanics Controls Cell Adhesion and Expansion on Low-Viscosity Liquids

Dexu Kong[1,2], **William Megone**[1,2], **Khai D. Q. Nguyen**[1,2], **Stefania Di Cio**[1,2], **Madeleine Ramstedt**[3] **and Julien E. Gautrot**[1,2*]

[1]*Institute of Bioengineering and* [2]*School of Engineering and Materials Science, Queen Mary, University of London, Mile End Road, London, E1 4NS, UK.*

[3]*Department of Chemistry, Umeå University, SE-90187 Umeå, Sweden.*

[*]*Corresponding author. j.gautrot@qmul.ac.uk*

Abstract

Adherent cell culture typically requires cell spreading at the surface of solid substrates to sustain the formation of stable focal adhesions and assembly of a contractile cytoskeleton. However, a few reports have demonstrated that cell culture is possible on liquid substrates such as silicone and fluorinated oils, even displaying very low viscosities (0.77 cSt). Such behaviour is surprising as low viscosity liquids are thought to relax much too fast (< ms) to enable the stabilisation of focal adhesions (with lifetimes on the order of minutes to hours). Here we show that cell spreading and proliferation at the surface of low viscosity liquids are enabled by the self-assembly of mechanically strong protein nanosheets at these interfaces. We propose that this phenomenon results from the denaturation of globular proteins such as albumin, in combination with the coupling of surfactant molecules to the resulting protein nanosheets. We use interfacial rheology and AFM indentation to characterise the mechanical properties of protein nanosheets and associated liquid-liquid interfaces. We identify a direct relationship between interfacial mechanics and the association of surfactant molecules with proteins and polymers assembled at liquid-liquid interfaces. In addition, our data indicate that cells primarily sense in-plane mechanical properties of interfaces, rather than relying on surface tension to sustain spreading, as in the spreading of water striders. These findings demonstrate that bulk and nanoscale mechanical properties may be designed independently, to provide structure and regulate cell phenotype, therefore calling for a paradigm shift for the design of biomaterials in regenerative medicine.

Keywords

The culture of adherent cells is typically thought to require cell spreading at the surface of solid or viscoelastic substrates to sustain the formation of stable focal adhesions and the assembly of a contractile cytoskeleton[1]. Adhesion to solid substrates and hydrogels has been showed to modulate a wide range of cell phenotypes such as proliferation[2], apoptosis[3], differentiation[4-6], endocytosis, motility[2, 7] and spreading[8-10]. In addition, matrix adhesion and the physical properties of the extracellular environment regulate pathological phenotypes such as epithelial-mesenchymal transitions, invasion and metastasis in cancer[11-13]. However, cell adhesion and matrix bulk mechanics do not always directly correlate, as in the case of cells spreading on Sylgard 184 PDMS[14], the adhesion of cells to viscoelastic hydrogels[15] and soft nanofibres[16] or in the remodelling of 3D cell-degradable hydrogels[17]. In such cases, it was proposed that other nano- to micro-scale properties of the cellular microenvironment (e.g. ECM remodelling or tethering, viscoelasticity and clustering of ligands) is responsible to such effects. However, this did not fully explain why cells failed to respond to the mechanical properties of Sylgard 184 PDMS with a wide range of mechanical properties. Recently, we even reported that uncrosslinked liquid PDMS supported cell adhesion and proliferation[18]. Similarly, Keese and Giaever previously reported the proliferation of fibroblasts at the surface of fluorinated and silicone oils[19, 20]. Adhesion and proliferation of anchorage-dependent cells was also reported at the surface of Pickering emulsions, although it was mediated in this case by a relatively thick (μm) coat of particles stabilising the corresponding interfaces[21]. Direct cell adhesion to liquid surfaces is surprising as low viscosity liquids are thought to relax much too fast (stress relaxation timescale < ms) to enable the stabilisation of focal adhesions (with lifetimes on the order of minutes to hours[22]). This suggested either the occurrence of very different mechanisms sustaining cell adhesion and proliferation at liquid interfaces compared to solid substrates, as in the integrin-independent migration of leukocytes[23], or the formation of a mechanically strong and elastic interface at the boundary between the two liquids (oil and cell culture medium). Here we show that cell adhesion and proliferation at the surface of low viscosity liquids are enabled by the self-assembly of mechanically strong nanoscale protein layers, protein nanosheets, at these interfaces. We characterise the physico-chemical properties of associated nanosheets and interfaces via interfacial rheology, X-ray photoelectron spectroscopy, Fourier Transform Infrared spectroscopy, Scanning Electron Microscopy and AFM indentation. Our results offer opportunities for rational design of liquid-liquid interfaces that support cell adhesion and proliferation and can be applied in stem cell technologies and regenerative medicine.

We first set out to determine some of the parameters regulating the proliferation of HaCaT cells at the surface of low viscosity oils, using the fluorinated oil Novec 7500 as a model system (Fig. 1). We observed a clear correlation between HaCaT proliferation and the concentration of the co-surfactant pentafluorobenzoyl chloride (PFBC, Fig. 1), to levels comparable to those observed on tissue culture

polystyrene (TPS). In addition, the growth profile of HaCaTs on fluorinated oil containing 10 and 5 μg/mL of surfactant and conditioned with bovine serum albumin (BSA) closely matched that of cells cultured on TPS (Fig. 2A). Indeed, cells cultured on these interfaces formed large spread colonies, similar in size and morphologies to those formed by HaCaTs on TPS. Cells growing at the interfaces remained viable and cell death levels remained comparable to those observed on TPS (Supplementary Fig. 1). In contrast, when cells were cultured on oil interfaces without surfactant, but conditioned with serum or BSA, only a few round colonies were observed (Fig. 1) and these were associated with higher occurrence of cell death (Supplementary Fig. S1). In addition, the bimodal dependence of HaCaT proliferation as a function of surfactant concentration, with a sharp drop above PFBC concentrations of 0.01 mg/mL, is proposed to result from the acidity of the surfactant used (PFBC is an acyl chloride). Indeed PFBC was found to lower the pH of the medium at increasing concentrations of PFBC (it remained at 7.5 after 24 h incubation with PFBC oil solutions at concentrations of 0.01 mg/mL or below but decreased to 7.2 at a concentration of 0.1 mg/mL and then continued to drop sharply to 6.5 and 2.0 at concentrations of 1 and 10 mg/mL, respectively). HaCaT proliferation was also observed in the case of interfaces conditioned with medium[18], but was surprisingly reduced on those conditioned with collagen (Supplementary Fig. S1).

In addition, we observed a similar phenomenon for the proliferation of HaCaT cells at the surface of silicone oils, in a viscosity-independent manner (in the range of 10-5000 cSt, Fig. 2B). Cells formed large and spread colonies on all silicone oils tested, when supplemented with the surfactant octanoyl chloride, whereas very few cells were observed on oils without surfactant (not even rounded colonies). The lack of contribution of the viscoelastic properties of the underlying substrate on cell proliferation, implicated in regulating cell spreading in other contexts[15, 24], implied the formation of a relatively strong mechanical interface between the two liquids. Overall, our results with protein-conditioned interfaces suggested that the surfactant-assisted assembly of proteins to hydrophobic fluid interfaces is required to allow cell adhesion and proliferation.

In order to investigate further the process of protein adsorption to oil interfaces, we used interfacial rheology[25, 26] to monitor associated changes in shear mechanical properties at the oil/buffer interface. In our set up, a De Nouy ring with a diamond-shape cross-section is placed at the liquid-liquid-interface and coupled to a rheometer. Oscillatory displacements are applied to quantify the shear properties of interfaces prior, during and post-assembly of protein nanosheets. The interfacial shear storage modulus of oil-buffer interfaces remained low (10^{-5}-10^{-4} N/m) and relatively insensitive to the surfactant concentration (Fig. 3A and Supplementary Fig. S2). Upon addition of BSA, the storage modulus increased by 2 to 5 orders of magnitude, depending on the surfactant concentration. The

time sweep profile of such adsorption followed two main stages, in agreement with previous reports of protein adsorption at oil-water interfaces[27-29]: a sharp increase in the storage modulus in the first 15-20 min, corresponding to the adsorption of proteins to the interface, followed by a strengthening stage, during which the storage modulus continued to increase modestly. In the case of the highest surfactant concentration tested (10 mg/mL), a second sharp increase in interfacial mechanics was observed during this strengthening stage, corresponding to the formation of multiple protein layers. Such processes were found to depend on the protein type and concentration as well as the presence of surfactants (although often resulting in the displacement of proteins from the interface[30]). Importantly, the BSA films formed at the oil-water interface were clearly strengthened (from 10^{-2}-10 N/m) as the surfactant concentration increased (Fig. 3A and Supplementary Fig. 2C). In addition, the interfacial loss modulus increased gradually as the PFBC concentration increased (Supplementary Fig. S2D), indicating slower relaxations of the corresponding interfaces. This trend correlated with a gradual increase in the content of fluorinated surfactant bound to the protein layer (up to 112 ± 11 surfactant/BSA molecule), as evidenced by XPS (Fig. 3A-C and Supplementary Fig. S3A). Indeed, XPS spectra clearly showed an increase in the F content as the PFBC concentration was raised, despite repeated washing of the interfaces with several solvents to remove soluble small molecules and solvents. This indicates that PFBC strongly interacts and is bound to the assembled protein nanosheets.

The presence of surfactants was also identified by FTIR, as protein assemblies displayed several bands in the region 1100-1250 cm^{-1}, corresponding to C-F stretching modes[31] (Fig. 3D and Supplementary Fig. S3B and C). In addition, FTIR provided evidence for the covalent coupling of surfactants to protein molecules, via the shoulder observed at 1720 cm^{-1}, corresponding to C=O stretching of esters. The shift in the amide I (1640-1660 cm^{-1}) and amide II (1520-1535 cm^{-1}) bands and the change in the ratio of their intensity indicated a reorganisation of the protein structure and its unfolding at the oil surface[32]. Therefore, our data indicate that globular proteins such as BSA can unfold and assemble to fluorophilic liquids, as is known to occur on solid substrates and at the surface of other hydrophobic liquids. This phenomenon itself is associated with an increase in the interfacial shear modulus of the system, but is strengthened in the presence of PFBC. It is proposed that acyl chlorides such as PFBC can react with proteins assembled at the interface and may provide hydrophobic crosslinks that contribute to this strengthening (Fig. 3E). However, it is also possible that the increased hydrophobicity of the resulting conjugated protein nanosheets results in a partial dehydration that leads to the increased in shear moduli.

The thickness of protein assemblies was characterised to determine whether these structures remained quasi-2D sheets or whether a more extended 3D morphology was achieved. Oil-in-buffer emulsions were deposited on silicon substrates and collapsed upon drying, leaving wrinkled skins corresponding to two proteins layers, as observed by SEM (Fig. 4 A). Protein nanosheets were observed for interfaces generated in the presence of PFBC, as well as in the case of interfaces generated by direct adsorption of BSA on oils without PFBC (Supplementary Fig. S4). Hence BSA denaturation is sufficient to maintain a cohesive mechanically strong protein nanosheet at liquid-liquid interfaces. The thickness of these protein sheets ranged from 14 ± 2 to 19 ± 2 nm, based on AFM characterisation (Fig. 4B/C and Supplementary Fig. S4). SEM characterisation of wrinkles afforded thicknesses in the range of 36 ± 5 to 57 ± 12 nm, slightly higher than those measured by AFM as SEM overestimates the cross-section of the double layer (Supplementary Fig. 4B-D). Overall, our results give direct evidence that BSA assembles at fluorinated oil interfaces into partially denatured protein layers. The hydrophobic PFBC present in the oil can then interact and incorporate within this protein layer and induces its crosslinking and strengthening (Fig. 3E), providing a suitable mechanical environment to sustain cell cycling.

The mechanism via which HaCaT cells sense interfacial mechanics was investigated next. Since BSA is unlikely to directly act as ligand for integrin binding in HaCaTs, we studied the impact of conditioning of BSA nanosheets by serum proteins. To do so, we labelled serum proteins using a fluorescent dye before exposing oil-in-water emulsions (Novec 7500 in PBS), stabilised by BSA (1 mg/mL) and PFBC (0.01 mg/mL). After exposure of the resulting emulsions to labelled serum, we indeed observed fluorescence at the periphery of droplets (Supplementary Fig. 5). Interestingly, this phenomenon was not associated with a change in the mechanical properties of interfaces, as interfacial rheology data did not show any additional increase in interfacial shear modulus upon exposure of a BSA/PFBC interface to serum (Supplementary Fig. 5A). Hence conditioning of BSA interfaces by serum proteins is proposed to enable cell adhesion and spreading to oil-water interfaces.

To further explore the mechanism via which cells sense mechanical properties at liquid-liquid interfaces, we considered that the inherent anisotropy of protein nanosheets deposited at liquid-liquid interfaces. Indeed, in-plane mechanics will be dominated by interfacial shear properties of protein nanosheets, whilst we propose that out-of-plane mechanics results from the combination of the elastic modulus and surface tension of the corresponding interface (Fig. 5A). Hence, depending on the precise molecular mechanism and dynamics controlling cell adhesion, cells may sense such anisotropy. Indeed, it was recently reported that cells exert traction forces resulting in out-of-plan deformations when spreading at the surface of soft hydrogels[33]. Similar forces could be exerted at

liquid-liquid interfaces and contribute to cell adhesion and spreading. To investigate whether cells are likely to sense the anisotropy of the liquid-liquid interfaces studied, we characterised the mechanical properties of interfaces via colloidal AFM indentation (hence normal to the plane of the interface, Fig. 5B). We observed a reduction in the stiffness of the interface when PFBC or BSA were introduced, as would be expected from the associated reduction in surface tension. However, when combining the two and assembling BSA nanosheets at liquid-liquid interfaces, little additional changes were observed and interfacial stiffness remained relatively constant at increasing PFBC concentrations. In comparison, PFBC had a marked impact on the interfacial shear modulus of the corresponding interfaces (Fig. 3A). Hence, our results indicate that interfacial shear properties dominate cell adhesion and proliferation at liquid-liquid interfaces, with little contribution from surface tension. Therefore, cell spreading at the surface of liquids is not comparable to the walking of water striders on the surface of water ponds and is more akin to a gecko adhesion phenomenon, although through a different mechanism of activation.

Overall, our results demonstrate that the dimensions (15-20 nm dry for nanosheets) and mechanical properties of the protein assemblies studied are in good agreement with the thickness of focal adhesions (at which forces are transmitted from the cell cytoskeleton to the extra-cellular environment), in the range of a few tens of nanometers[34], and the thickness of actin stress fibres, also in the range of a few tens of nanometers (for bundles)[35]. Hence intracellular (FA and stress fibres) and extracellular (protein nanosheets) protein assemblies have comparable dimensions and their mechanical properties are expected to be comparable (extrapolated moduli for BSA nanosheets studied are in the range of 1-6 MPa, whilst stress fibres were reported to display MPa moduli[36]). Therefore, these observations are in very good agreement with the notion that shear forces exerted by cells can be counterbalanced by the strength of the nanosheets studied.

Cell adhesion to the ECM is an important process regulating the phenotype and function of many stem cells[37]. However, from an engineering and biotechnology point of view the requirement for hard, rigid substrates with strong bulk mechanical properties can be an important drawback. This is the case for the scale up of cell expansion systems and the fabrication of cell sheets. Hard rigid substrates also require enzymatic digestion for cell recovery, which can be harmful or induce changes in cell phenotype (harsh trypsin treatment decreases the colony forming efficiency of keratinocytes[38]). Our study demonstrates that cell proliferation and culture can be particularly effective at liquid-liquid interfaces, despite the absence of bulk mechanical properties of the culture substrate. The use of liquid substrates may be used to directly addresses scale up and cell detachment issues, by passing the use of solid substrates. In addition, cell culture on liquid substrates may find further application in

other biotechnological platforms such as microdroplet systems, which have been restricted by the requirements of cell adhesion[39]. Finally, the design of biomaterials and implants should benefit from the concept that cell adhesion phenomena can be engineered at interfaces independently of other bulk properties that may be required to confer flexibility or structure.

Supporting Information. Materials and methods, cell viability assays, statistical analysis reports and additional interfacial rheology, XPS, FTIR, AFM and SEM.

Author Contributions. The experiments were designed by J.E.G. and D.K. and carried out by D.K. K.D.Q.N. carried out some of the interfacial rheology experiments and designed associated methodologies. S.D.C. carried out AFM characterisation. M.R. carried out XPS characterisation. W.M. carried out AFM indentation experiments. All authors have given approval to the final version of the manuscript.
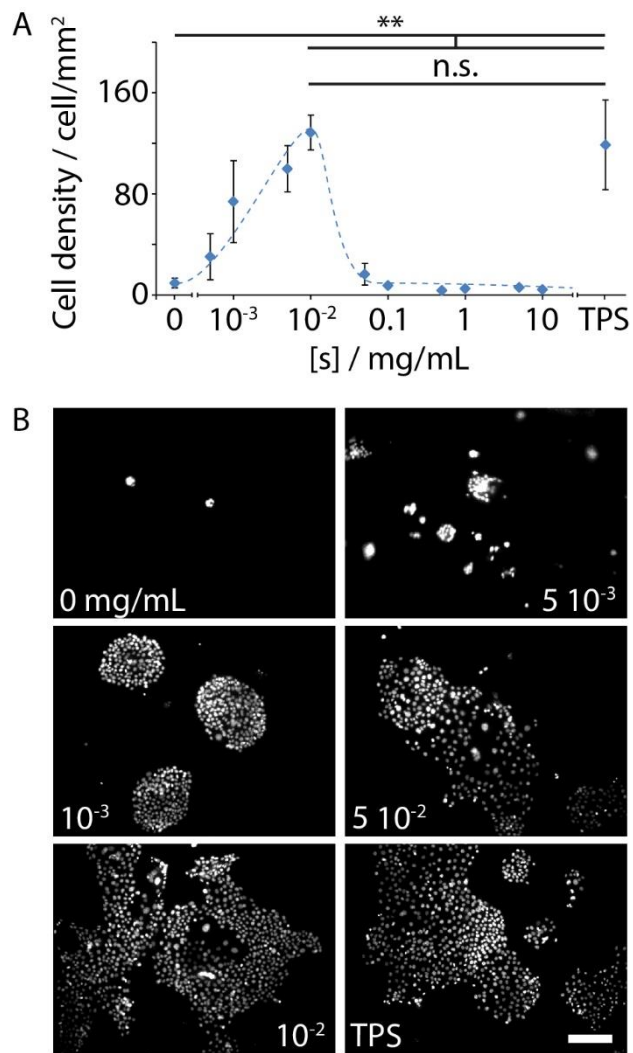
Figure 1. Cell proliferation on low viscosity liquids is mediated by surfactants. A. HaCaT cells proliferation on a fluorinated oil (Novec 7500, 0.77 cSt) containing the surfactant pentafluorobenzoyl chloride, PFBC, at different concentrations (conditioning with medium). [S]: surfactant concentration. Error bars are s.e.m.; n=3. B. Corresponding images of nuclear stainings (Hoechst, scale bars are 200 μm).
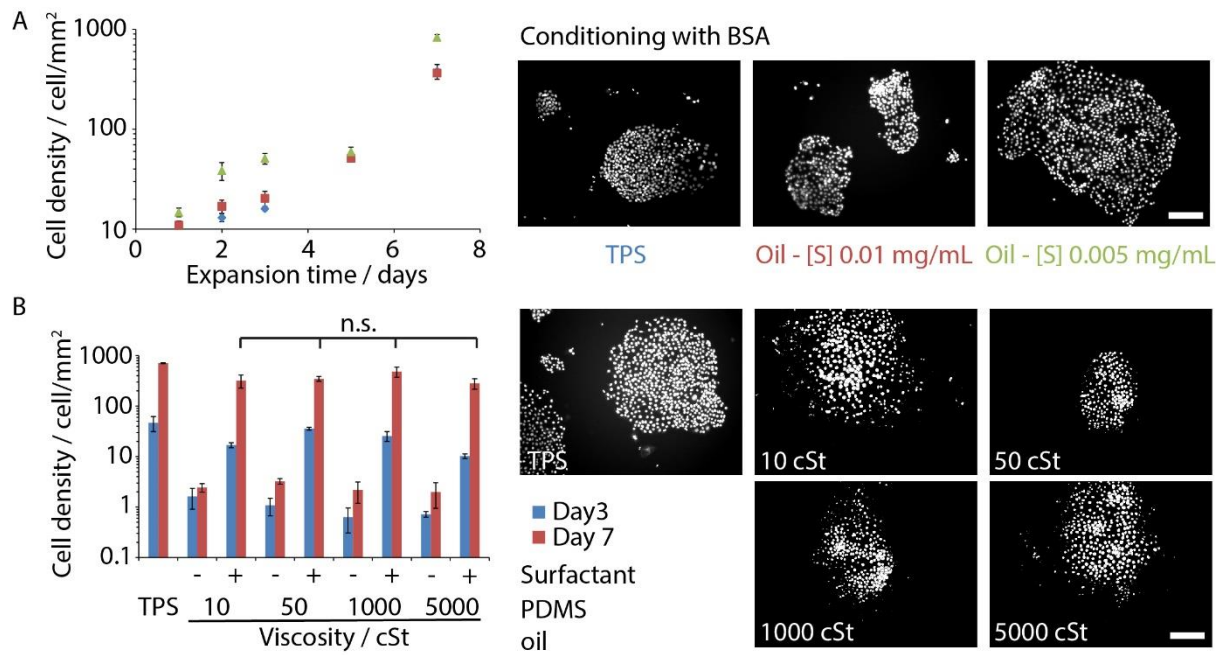
Figure 2. Impact of surface conditioning and oil viscosity on HaCaT proliferation. A. HaCaT cell proliferation profile on interfaces conditioned with BSA (1 mg/mL; blue diamonds, TPS; red square, Novec 7500 + 0.01 mg/mL PFBC; green triangles, Novec 7500 + 0.005 mg/mL PFBC). B. HaCaT cell proliferation on silicone oils with viscosities in the range of 10-5000 cSt and conditioned with BSA (1mg/mL; blue, Day 3; red, Day 7; TPS, tissue culture polystyrene; '-', no surfactant added; '+', 0.5 mg/mL octanoyl chloride added; 5000/1000/50/10 describe the viscosity (cSt) of the PDMS oil used). Error bars are s.e.m.; n=3. Images are corresponding nuclear stainings (Hoechst, scale bars are 200 μm).
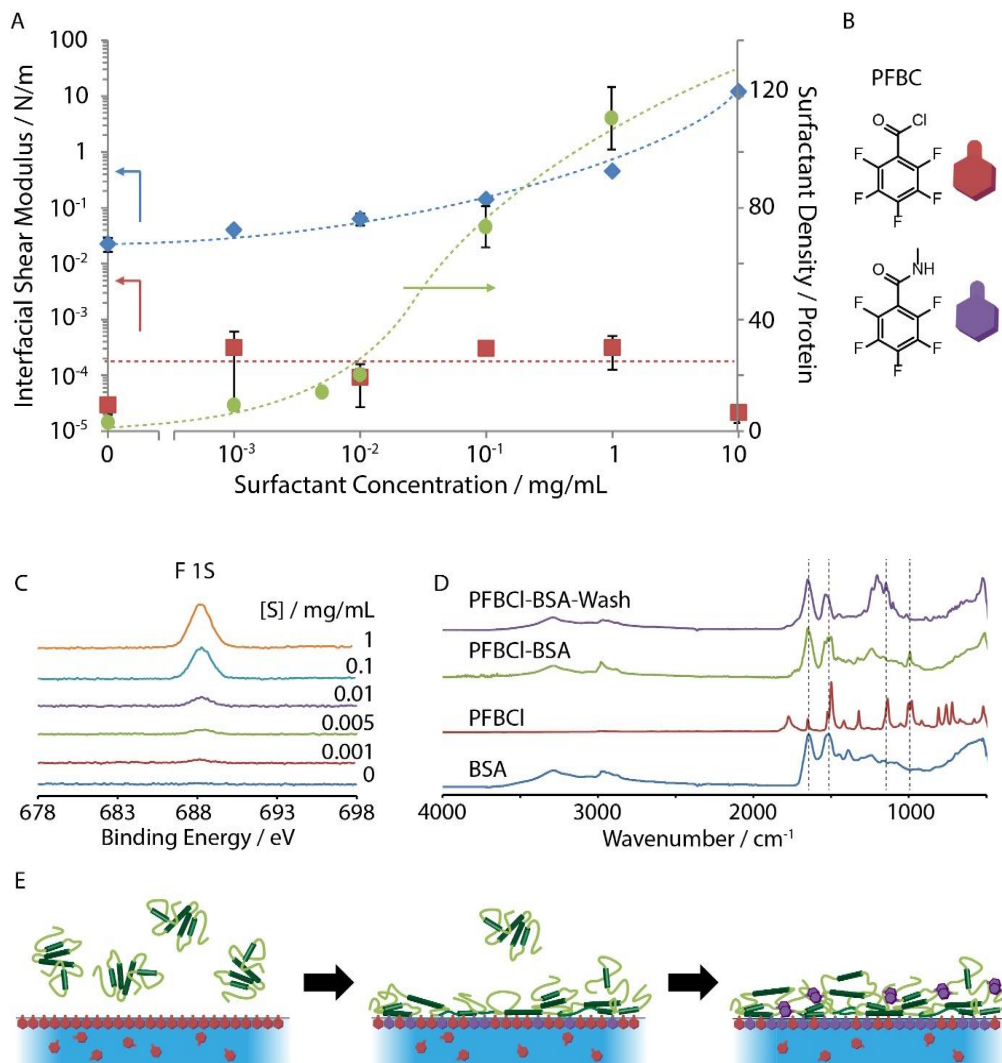
Figure 3. Protein adsorption at the surface of fluorinated oils forms a strong nanoscale mechanical interface. A. Evolution of interfacial shear moduli and surfactant composition as a function of PFBC concentration. Red squares and blue diamonds are the interfacial shear moduli before and after the adsorption of BSA (1 mg/mL), respectively (error bars are s.e.m.; n=3). Green triangles are the surfactant compositions of protein assemblies determined from XPS (expressed as number of surfactant/BSA protein; error bars are experimental errors, 10%; the dotted lines are only intended as a guide to the eye). B. Structure of PFBC and the structure of PFBC covalently bound to proteins via amides. C. XPS spectra (F 1S) obtained for dried emulsions generated with Novec 7500 (different concentrations of PFBC surfactant [S]) and BSA (1 mg/mL). See the methods section for details of functionalisation calculations and Supplementary Fig. S3 for C 1S spectra. D. FTIR spectra obtained for pristine BSA, PFBC, protein films generated in emulsions (10 mg/mL PFBC and 1 mg/mL BSA) before (PFBC-BSA) and after (PFBC-BSA-wash) washing with ethanol (see Fig. S3 for zooms of part of these spectra). E. Schematic representation of protein deposition at oil interfaces.
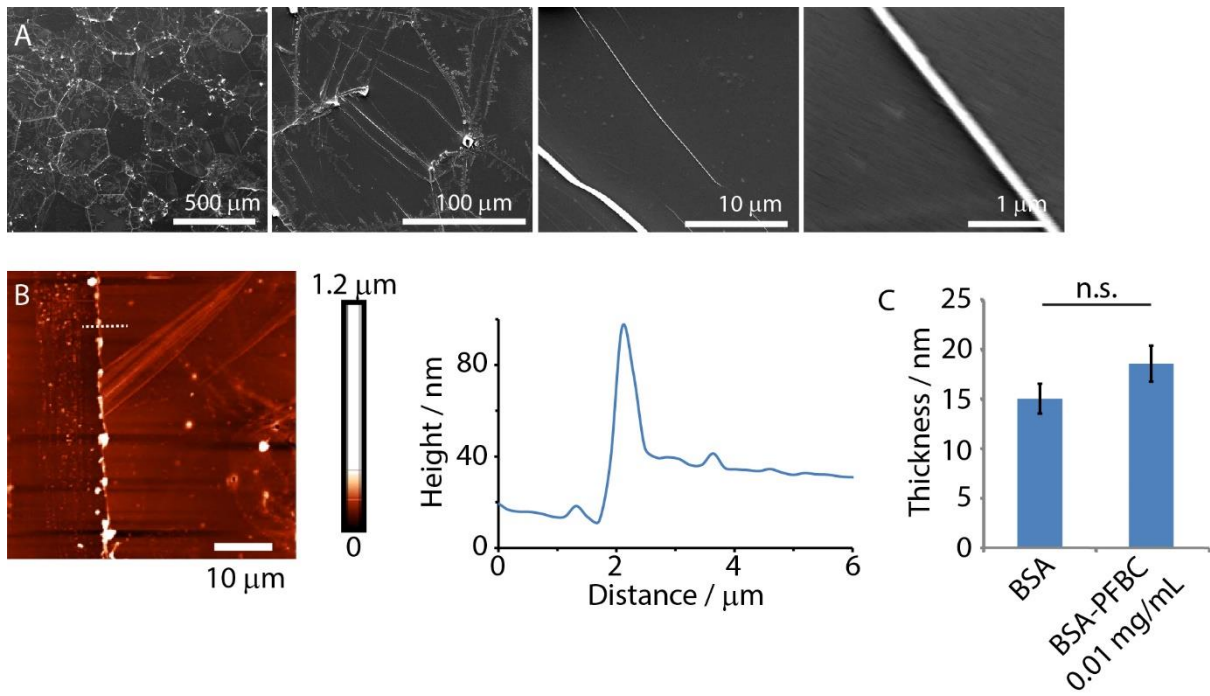
Figure 4. Characterisation of the self-assembled protein nanosheets. A. SEM images of oil droplets ([S] = 0.01 mg/mL, BSA = 1 mg/mL), dried onto silicon substrates. B. and C. AFM characterisation (height image, profile and quantification of thickness) of oil droplets ([S] = 0.01 mg/mL, BSA = 1 mg/mL), dried onto silicon substrates. Error bars are s.e.m.; n>50.
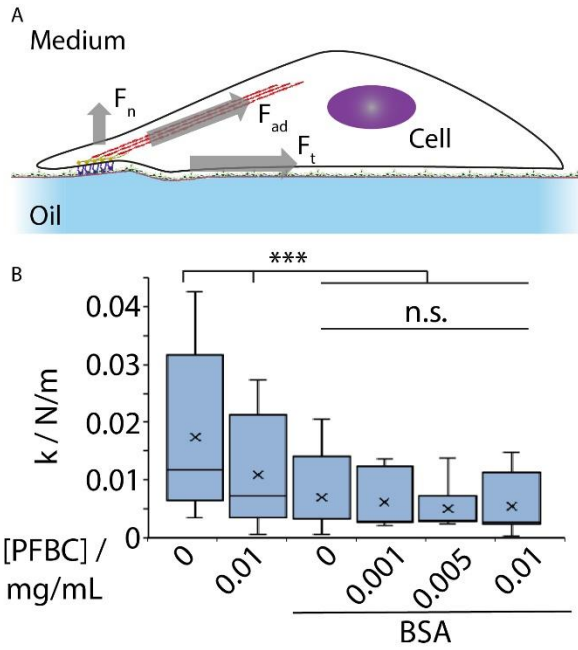
Figure 5. Characterisation of transverse mechanical properties of nanosheet-assembled interfaces.
A. Schematic representation of a cell applying forces across an oil-water interface in the normal and tangential directions. B. Stiffness of fluorinated oil–water interfaces with varying BSA and surfactant (PFBC) concentrations measured by interfacial AFM with a colloidal probe (indentation depths were between 500-1000 nm at a frequency of 1 Hz; error bars are s.e.m; n = 900).

References

(1)   Moore, S. W.; Roca-Cusachs, P.; Sheetz, M. P., *Cell* **2010,** *19,* 194-206.

(2)   Ulrich, T. A.; de Juan Pardo, E. M.; Kumar, S., *Cancer Res.* **2009,** *69*, 4167-4174.

(3)   Chen, C. S.; Mrksich, M.; Huang, S.; Whitesides, G. M.; Ingber, D. E., *Science* **1997,** *276*, 1425-1428.

(4)   Dalby, M. J.; Gadegaard, N.; Tare, R.; Andar, A.; Riehle, M. O.; Herzyk, P.; Wilkinson, C. D. W.; Oreffo, R. O. C., *Nat. Mater.* **2007,** *6*, 997-1003.

(5)   Saha, K.; Keung, A. J.; Irwin, E. F.; Li, Y.; Little, L.; Schaffer, D. V.; Healy, K. E., *Biophys. J.* **2008,** *95*, 4426-4438.

(6)   Engler, A. J.; Sen, S.; Sweeney, H. L.; Discher, D. E., *Cell* **2006,** *126*, 677-689.

(7)   Kim, S. N.; Jeibmann, A.; Halama, K.; Witte, H. T.; Walte, M.; Matzat, T.; Schillers, H.; Faber, C.; Senner, V.; Paulus, W.; Klambt, C., *Dev.* **2014,** *141*, 3233-3242.

(8)   Pelham, R. J.; Wang, Y.-L., *Proc. Natl. Acad. Sci.* **1997,** *94*, 13661-13665.

(9)   Tzvetkova-Chevolleau, T.; Stephanou, A.; Fuard, D.; Ohayon, J.; Schiavone, P.; Tracqui, P., *Biomaterials* **2008,** *29*, 1541-1551.

(10)   Yeung, T.; Georges, P. C.; Flanagan, L. A.; Marg, B.; Ortiz, M.; Funaki, M.; Zahir, N.; Ming, W.; Weaver, V.; Janmey, P. A., *Cell Motil. Cytoskeleton* **2005,** *60*, 24-34.

(11)   Levental, K. R.; Yu, H.; Kass, L.; Lakins, J. N.; Egeblad, M.; Erler, J.; Fong, S. F. T.; Csiszar, K.; Giaccia, A.; Weninger, W.; Yamauchi, M.; Gasser, D. L.; Weaver, V., *Cell* **2009,** *139*, 891-906.

(12)   Wei, S. C.; Fattet, L.; Tsai, J. H.; Guo, Y.; Pai, V. H.; Majeski, H. E.; Chen, A. C.; Sah, R. L.; Taylor, S. S.; Engler, A. J.; Yang, J., *Nat. Cell Biol.* **2015,** *17*, 678-688.

(13)   Chaudhuri, O.; Koshy, S. T.; Branco da Cunha, C.; Shin, J.-W.; Verbeke, C. S.; Allison, K. H.; Mooney, D. J., *Nat. Mater.* **2014,** *13*, 970-978.

(14)   Trappmann, B.; Gautrot, J. E.; Connelly, J.; Strange, D. G. T.; Li, Y.; Oyen, M. L.; Cohen Stuart, M. A.; Boehm, H.; Li, B.; Vogel, V.; Spatz, J. P.; Watt, F. M.; Huck, W. T. S., *Nat. Mater.* ***2012,*** *11*, 642-649.

(15)   Chaudhuri, O.; Gu, L.; Darnell, M.; Klumpers, D.; Bencherif, S. A.; Weaver, J. C.; Huebsch, N.; Mooney, D. J., *Nat. Commun.* **2015,** *6*, 6364.

(16)   Baker, B. M.; Trappmann, B.; Wang, W. Y.; Sakar, M. S.; Kim, I. L.; Shenoy, V. B.; Burdick, J. A.; Chen, C. S., *Nat. Mater.* **2015,** *14*, 1262-1268.

(17)   Khetan, S.; Guvendiren, M.; Legant, W. R.; Cohen, D. M.; Chen, C. S.; Burdick, J. A., *Nat. Mater.* **2013,** *12*, 458-465.

(18)   Kong, D.; Nguyen, K. D. Q.; Megone, W.; Peng, L.; Gautrot, J. E., *Faraday Discuss.* **2017,** *204*, 367-381.

(19)   Giaever, I.; Keese, C. R., *Proc. Natl. Acad. Sci.* **1983,** *80*, 219-222.

(20)   Keese, C. R.; Giaever, I., *Science* **1983,** *219*, 1448-1449.

(21)   Pan, M.; Rosenfeld, L.; Kim, M.; Xu, M.; Lin, E.; Derda, R.; Tang, S. K. Y., *ACS Appl. Mater. Interfaces* **2014,** *6*, 21446-21453.

(22)   Gardel, M. L.; Schneider, I. C.; Aratyn-Schaus, Y.; Waterman, C. M., *Annu. Rev. Cell Dev. Biol.* **2010,** *26*, 315-333.

(23)   Lammermann, T.; Bader, B. L.; Monkley, S. J.; Worbs, T.; Wedlich-Soldner, R.; Hirsch, K.; Keller, M.; Forster, R.; Critchley, D. R.; Fassler, R.; Sixt, M., *Nature* **2008,** *453*, 51-55.

(24)   Kourouklis, A. P.; Lerum, R. V.; Bermudez, H., *Biomaterials* **2014,** *35*, 4827-4834.

(25)   Fuller, G. G.; Vermant, J., *Annu. Rev. Chem. Biomol. Eng.* **2012,** *3*, 519-543.

(26)   Bos, M. A.; van Vliet, T., *Adv. Colloid. Interf. Sci.* **2001,** *91*, 437-471.

(27)   Baldursdottir, S. G.; Fullerton, M. S.; Nielsen, S. H.; Jorgensen, L., *Colloid Surf. B Biointerfaces* **2010,** *79*, 41-46.

(28)   Freer, E. M.; Yim, K. S.; Fuller, G. G.; Radke, C. J., *J. Phys. Chem. B* **2004,** *108*, 3835-3844.

(29)   Campana, M.; Hosking, S. L.; Petkov, J. T.; Tucker, I. M.; Webster, J. R. P.; Zarbakhsh, A.; Lu, J. R., *Langmuir* **2015,** *31*, 5614-5622.

(30)   Wilde, P. J.; Clark, D. C., *J. Colloid Interface Sci.* **1993,** *155*, 48-54.

(31) Bellamy, L. J., *The infrared spectra of complex molecules*. Wiley: New York, 1959.

(32) McClellan, S. J.; Franses, E. I., *Colloid. Surf. A: Physicochem. Eng. Aspects* **2005,** *260*, 265-275.

(33) Legant, W. R.; Choi, C. K.; Miller, J. S.; Shao, L.; Gao, L.; Betzig, E.; Chen, C. S., *Proc. Natl. Acad. Sci.* **2013,** *110*, 881-886.

(34) Kanchanawong, P.; Shtengel, G.; Pasapera, A. M.; Ramko, E. B.; Davidson, M. W.; Hess, H. F.; Waterman, C. M., *Nature* **2010,** *468*, 580-584.

(35) Blanchoin, L.; Boujemaa-Paterski, R.; Sykes, C.; Plastino, J., *Physiol. Rev.* **2014,** *94*, 235-263.

(36) Deguchi, S.; Ohashi, T.; Sato, M., *J. Biomech.* **2006,** *39*, 2603-2610.

(37) Discher, D. E.; Mooney, D. J.; Zandstra, P. W., *Science* **2009,** *324*, 1673-1677.

(38) Jones, P. H.; Watt, F. M., *Cell* **1993,** *73*, 713-724.

(39) Huebner, A.; Sharma, S.; Srisa-Art, M.; Hollfelder, F.; Edel, J. B.; deMello, A. J., *Lab Chip* **2008,** *8*, 1244-1254.